Evaluation of Bearing Capacity of Footing Strip Based on Node-Based Smoothed Finite Element Method and Conic Programming

Tran Vu Hoang
University of Technology, Ho Chi Minh City, Vietnam
vuhoangtran151189@gmail.com

Hoang C. Nguyen
University of Technology, Ho Chi Minh City, Vietnam
nchoangoxf@gmail.com

Giang H.Ong
International University, Ho Chi Minh City, Vietnam
tgiangoh@gmail.com

Thanh T. Pham
University of Technology, Ho Chi Minh City, Vietnam
trithanh221@yahoo.com.vn

ABSTRACT

In this paper, bearing capacity of footing resting is evaluated by using upper bound analysis. The soil is modelled by a perfectly-plastic Mohr-Coulomb model. Node-based smoothed finite element method (NS-FEM) is used to approximate the kinematically admissible velocity fields. Then optimisation problem is formulated as a problem of minimising a sum of Euclidean norms so that it can be solved using an efficient second order cone programming (SOCP) algorithm in order to determine collapse load and failure mechanism as well.

Key Words: *Upper bound limit analysis, Bearing capacity, NS-FEM, SOCP*

INTRODUCTION

Limit analysis has been using as a powerful tool to determine many kinds of geotechnical problems such as the ultimate load, failure mechanism of structures as well as the stability of slopes. The upper bound theorem of limit analysis states that the power dissipated by any kinematically admissible velocity field can be equated to the power dissipated by the external loads in order to give a rigorous upper bound on the actual limit load. More information of limit theorems formulation of mechanical problems can be found in various resources (Le, Gilbert & Askes, 2009; Le, Nguyen-Xuan & Nguyen-Dang, 2010; Le, Askes, Gilbert, 2010).

In general, two main elements of any limit analysis procedure are discretisation method and optimisation algorithm. At first, kinematically admissible velocity fields, which satisfy compatibility, the flow rule and velocity boundary conditions,

can be approximated using various computational methods. In this paper, these kinematic fields will be approximated by node-based smoothed finite elements method (NS-FEM). After that, a suitable optimisation problem is formulated in order to apply mathematical programming techniques. Once the displacement or stress fields are approximated and the bound theorems of plasticity are applied, limit analysis becomes a problem of optimisation involving either linear or nonlinear programming. This can be solved using linear or non-linear programming techniques which are integrated in commercial or in-house optimisation packages. In this paper, the underlying optimisation problem will be modelled in the form of a standard second-order cone programming so that it can be solved efficiently using available primal-dual interior point algorithms. In this research, we use a software called Mosek (Mosek, 2011) in order to conduct the optimization procedure.

BRIEF OF THE NS-FEM

The NS-FEM is one of several models of the smoothed finite element methods (Smoothed-FEM).Each model effectively deal with a specific problem in mechanics. More details of this model as well as smoothed-FEM can be found in Liu's Book (Liu & Nguyen Thoi Trung, 2010).

In NS-FEM, based on the mesh of elements, we further discretise the problem domain into smoothing domains based on each node of the mesh by connecting portions of surrounding elements sharing the node.

In detail, for node-based smooth FEM the smoothing domain is created by connecting sequentially the mid-edge point to the central points of the surrounding elements sharing node. The problem domain Ω is discretised using N_e elements with N_n nodes, such that $\Omega = \sum_{i=1}^{Ne} \Omega_i^e$ and $\Omega_i^e \cap \Omega_j^e, i \neq j$.

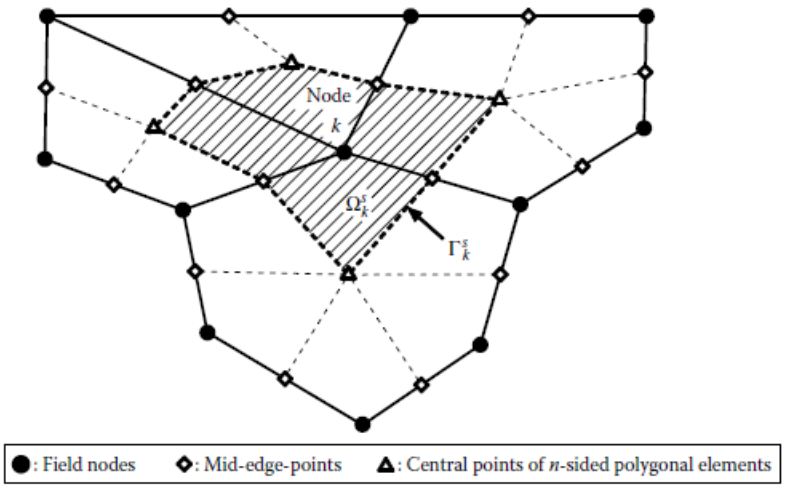

Figure 1: Illustration of node-based discretisation

For T3 or T4 elements which are popularly used, the shape function for NS-FEM is the same as FEM. However, the compatible strain field is replaced with the smoothed strain field over the smoothing domains:

$$\tilde{\varepsilon}(x) = \boldsymbol{L}_d \overline{\boldsymbol{u}} = \boldsymbol{L}_d \left(\sum_{I=1}^{N_n} \boldsymbol{N}_I(x) \overline{\boldsymbol{d}}_I \right) = \sum_{I=1}^{N_n} \boldsymbol{L}_d \boldsymbol{N}_I(x) \overline{\boldsymbol{d}}_I = \sum_{I=1}^{N_n} \tilde{\boldsymbol{B}}_I \overline{\boldsymbol{d}}_I \quad (1)$$

Where

$$\tilde{\boldsymbol{B}}_I = \boldsymbol{L}_d \boldsymbol{N}_I(x) \quad (2)$$

For general polygonal elements, using the linear PIM technique to determine the smoothed shape functions .The linear system equation of NS-FEM has the form:

$$\overline{\boldsymbol{K}}^{NS\text{-}FEM} \overline{\boldsymbol{d}} = \overline{\boldsymbol{f}} \quad (3)$$

In which, $\overline{\boldsymbol{K}}^{NS\text{-}FEM}$ is the smoothed stiffness matrix whose entries are given by:

$$\overline{\boldsymbol{K}}_{IJ}^{NS-FEM} = \int_{\Omega} \overline{\boldsymbol{B}}_I^T c \overline{\boldsymbol{B}}_J \, d\Omega = \sum_{k=1}^{N_n} \int_{\Omega_k^s} \overline{\boldsymbol{B}}_I^T c \overline{\boldsymbol{B}}_J \, d\Omega = \sum_{k=1}^{N_n} \overline{\boldsymbol{B}}_I^T c \overline{\boldsymbol{B}}_J \, A_k^s \quad (4)$$

Note that $\overline{\boldsymbol{B}}_J$ is constant in Ω^s_k and A^s_k is the area of node-based domain and $\overline{\boldsymbol{B}}_I$ is computed using equation:

$$\overline{\boldsymbol{B}}_I = \frac{1}{A_k^s} \int_{\Gamma_k^s} \boldsymbol{L}_n(x) \boldsymbol{N}_I(x) d\Gamma = \begin{bmatrix} \overline{b}_{Ix} & 0 \\ 0 & \overline{b}_{Iy} \\ \overline{b}_{Iy} & \overline{b}_{Ix} \end{bmatrix} \quad (5)$$

With

$$\overline{b}_{Ih} = \frac{1}{A_k^s} \int_{\Gamma_k^s} n_h(x) \mathbf{N}_\mathbf{I}(\mathrm{x}) d\Gamma, h = x, y. \quad (6)$$

It is worth noting that the NS-FEM is different from the standard FEM by two key points: (1) FEM uses the compatible strain on the element, while NS-FEM uses the smoothed strain on the smoothing domain; and (2) the assembly process of FEM is based on elements, while that of NS-FEM is based on smoothing domain Ω_k

Application of standard FEM can be found in paper of Sloan (Sloan & Kleeman, 1995). However, assumptions used in standard FEM formulation are not always relevant for different kind of problems.

UPPER BOUND LIMIT ANALYSIS FORMULATION

Consider a rigid-perfectly plastic body of area $\Omega \in \mathrm{P}^2$ with boundary Γ, which is subjected to body forces $\mathbf{f}$ and to surface tractions $\mathbf{g}$ on the free portion Γ_t of Γ.

The constrained boundary Γ_u is fixed and $\Gamma_u \cup \Gamma_t = \Gamma$, $\Gamma_u \cap \Gamma_t = \%$. Let $\dot{\mathbf{u}}$ be plastic velocity or flow fields that belong to a space Y of kinematically admissible velocity fields. The strain rates ε can be expressed by relations

$$\boldsymbol{\varepsilon} = \begin{bmatrix} \dot{\varepsilon}_{xx} \\ \dot{\varepsilon}_{yy} \\ \dot{\gamma}_{xy} \end{bmatrix} = \nabla \dot{\mathbf{u}} \tag{7}$$

With is the differential operator:

$$\nabla = \begin{bmatrix} \dfrac{\partial}{\partial x} & 0 \\ 0 & \dfrac{\partial}{\partial y} \\ \dfrac{\partial}{\partial y} & \dfrac{\partial}{\partial x} \end{bmatrix} \tag{8}$$

The external work rate associated with a virtual plastic flow $\dot{u}$ in the linear form as:

$$W_{ext}(\dot{\mathbf{u}}) = \int_{\Omega} \mathbf{f}^T \dot{\mathbf{u}} \mathrm{d}\Omega + \int_{\Gamma_t} \mathbf{g}^T \dot{\mathbf{u}} \mathrm{d}\Gamma \tag{9}$$

The internal plastic dissipation of the two-dimensional domain Ω can be written as:

$$W_{int}(\varepsilon) = \int_{\Omega} D(\varepsilon) \mathrm{d}\Omega \tag{10}$$

Where the plastic dissipation $D(\dot{\varepsilon})$ is defined by:

$$D(\boldsymbol{\varepsilon}) = \max_{\psi(\sigma) \le 0} \sigma : \varepsilon \equiv \sigma_{\varepsilon} : \varepsilon \tag{11}$$

with σ represents the admissible stresses contained within the convex yield surface $\psi(\sigma)$ and σ_{ε} represents the stresses on the yield surface associated to any strain rates ε through the plasticity condition.

The kinematic theorem of plasticity states that the structure will collapse if and only if there exists a kinematically admissible displacement field $\dot{\mathbf{u}} \in Y$, such that:

$$W_{int}(\boldsymbol{\varepsilon}) < \lambda^{+} W_{ext}(\dot{\mathbf{u}}) + W_{ext}^{0}(\dot{\mathbf{u}}) \tag{12}$$

If defining $X = \{\dot{\mathbf{u}} \in Y | W_{ext}(\dot{\mathbf{u}}) = 1\}$, the collapse load multiplier λ^{+} can be determined by the following mathematical programming

$$\lambda^{+} = \min_{\dot{\mathbf{u}} \in C} \int_{\Omega} D(\dot{\varepsilon}) \mathrm{d}\Omega - W_{\mathrm{ext}}^{0}(\dot{\mathbf{u}}) \tag{13}$$

NS-FEM FORMULATION FOR PLANE STRAIN WITH MORH - COULOMB YIELD CRITERION:

In this study, the Mohr-Coulomb criterion is used:

$$\psi(\sigma) = \sqrt{(\sigma_{xx} - \sigma_{yy})^2 + 4\tau_{xy}} + (\sigma_{xx} + \sigma_{yy})\sin\varphi' - 2c\cos\varphi' \tag{14}$$

The plastic strains are assumed to obey the normality rule:

$$\varepsilon = \dot{\lambda}\frac{\partial\psi}{\partial\sigma} \tag{15}$$

Where the plastic multiplier $\dot{\lambda}$ is non – negative. Therefore, the power of dissipation can be formulated as a function of strain rates for each domain:

$$D(\dot{\varepsilon}) = cA_i t_i \cos\varphi' \tag{16}$$

Where

$$\left\| \rho_i \right\| \le t_i \tag{17}$$

$$\rho_i = \begin{bmatrix} \rho_{1i} \\ \rho_{2i} \end{bmatrix} = \begin{bmatrix} \dot{\varepsilon}_{xx} - \dot{\varepsilon}_{yy} \\ \dot{\gamma}_{xy} \end{bmatrix} \tag{18}$$

$$\dot{\varepsilon}_{xx} - \dot{\varepsilon}_{yy} = t_i \sin\varphi' \tag{19}$$

Introducing an approximation of the displacement and using the smoothed strains, the upper bound limit analysis problem for plane strain can be formulated as:

$$\lambda^+ = \min \sum_{j=1}^{Nnode} cA_i t_i \cos\varphi' \tag{20}$$

$$s.t\begin{cases} \dot{\mathbf{u}}^h = \mathbf{0} & on\ \Gamma_u \\ W_{ext}(\dot{\mathbf{u}}^h) = 1 & \\ \left\| \rho_i \right\|_i \le t_i & i = 1,2,\mathrm{K}\ , N_{node} \end{cases} \tag{21}$$

Where N_{node} is the number of node of the whole investigated domain.

NUMERICAL EXAMPLE

Bearing capacity factor Nc

In this section, the performance of the new upper bound formulation is assessed by applying it to predict the collapse load for a plane strain strip footing. The exact collapse load for a strip footing on a weightless soil N_c was given in by Prandtl (Prandlt, 1920), thereby enabling objective validation.

Undrained loading of a rigid strip footing

The exact collapse pressure q_{ult} for a smooth rigid strip footing on a purely cohesive soil may be expressed as $q_{ult} = cN_c$,where c is the un-drained shear strength and the bearing capacity factor $N_c = \pi + 2$ .Besides, due to symmetry only half of the foundation is considered. The rectangular region of $L = 5B$ and $H = 2B$ was considered sufficiently large to ensure that rigid elements show up along the entire boundary. The influence of the rigid footing is represented by a uniform vertical load and appropriate boundary conditions were applied as shown in Figure 2.

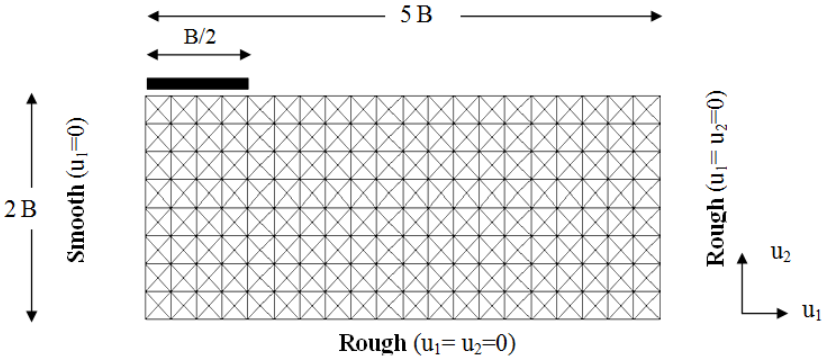

Figure 2: Finite element mesh and displacement boundary conditions

Table 1 lists results of N_c calculated by various meshes by NS-FEM. It can be clearly seen that with mesh of only 540 elements, the NS-FEM analysis provide us the result 5.3332, which is 3.72% error compared to the exact solution. Besides, the convergence rate to the exact solution is also very good. Running the analysis with finer meshes produces results rapidly approaching the exact solution. For example, mesh of 4860 elements provide approximation of N_c by 5.2036, only 1.2 % error compared to exact N_c

Table 1: Comparing error of the N_c approximation by NS-FEM in undrained condition

Number of Elements	540	960	1500	2160	2940	3840	4860
N_c	5.3332	5.2828	5.2544	5.2354	5.2216	5.2114	5.2036
Error(%)	3.73	2.75	2.19	1.82	1.56	1.36	1.21

Drained loading of a rigid strip footing

The Prandtl collapse pressure for a surface footing on a weightless cohesive-frictional soil is $q_{ult} = c' N_c$ where $N_c = [exp(\pi tan\,\varphi')tan\,2(\pi/4 + \frac{\varphi'}{2}) - 1]\cot\varphi'$,

c' and φ' are the effective cohesion and friction angle, respectively. The model solved is shown in Figure 3.

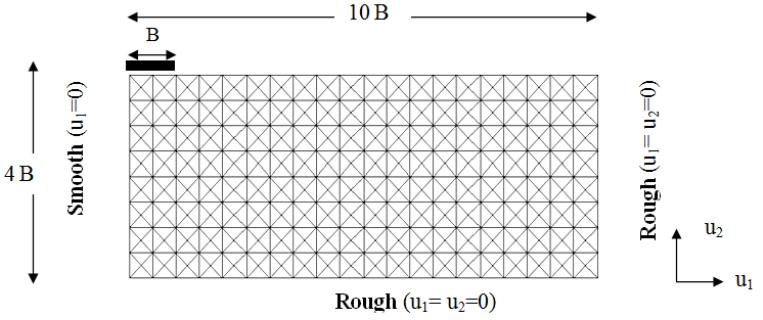

Figure 3: Finite element mesh and displacement boundary conditions

Several cases for internal friction angle φ' of this numerical problems are carried out in order to compare results with Prandtl's as well as Terzaghi's values (as shown in Figure 4 and Table 2).

Table 2: Comparing bearing capacity N_C in drained condition

Internal friction angle φ' (^{0})	Bearing capacity factor N_c		
	NS-FEM	Terzaghi	Prandt [6]
5	6.5942	7.34	6.48882
10	8.4626	9.60	8.34493
15	11.1044	12.86	10.9765
20	14.9756	17.69	14.8347
25	20.8711	25.13	20.7205
30	30.4406	37.16	30.1396
35	46.5213	57.75	46.1236
40	76.7604	95.69	75.3131
45	148.8791	172.29	133.874

As we can see in the graph above, NSFEM always provide better results for bearing capacity factor N_c than the results calculated by Terzaghi's procedure. It is obvious that errors in Terzaghi's results are higher than 10% for many cases of internal friction angle φ' and the gap between exact values calculated by Prandt and this procedure is expanding gradually when φ' is increasing. On the other hand, the N_c values approximated by NSFEM are lower (better-close to the Prandt's values) than Terzaghi's. Especially for φ' smaller than 40 degrees, NSFEM produce very good bearing capacity factor N_c which is only 1%-2% difference from the exact values.

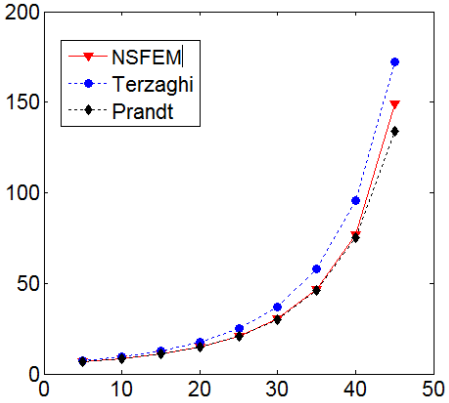

Figure 4: Bearing capacity Factor N_c

The patterns of plastic energy dissipation and velocity field are also shown in Figure 5.

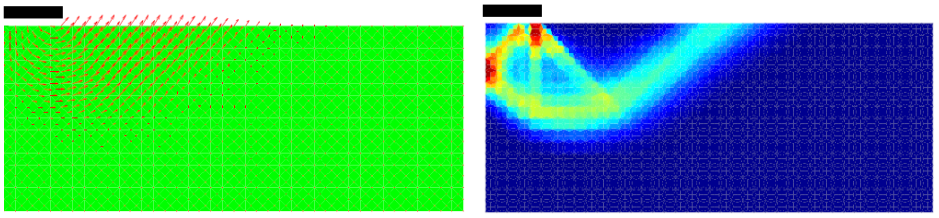

Figure 5.1 Patterns of plastic energy dissipation and velocity field $\varphi' = 20^0$

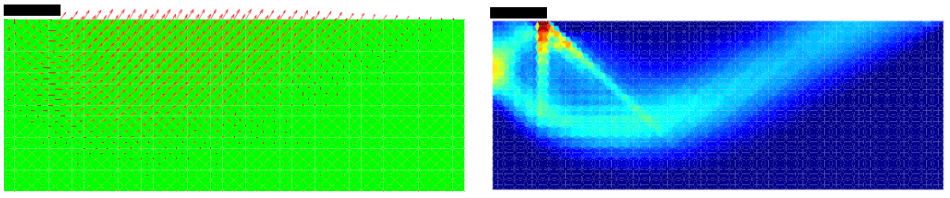

Figure 5.2 Patterns of plastic energy dissipation and velocity field $\varphi' = 30^0$

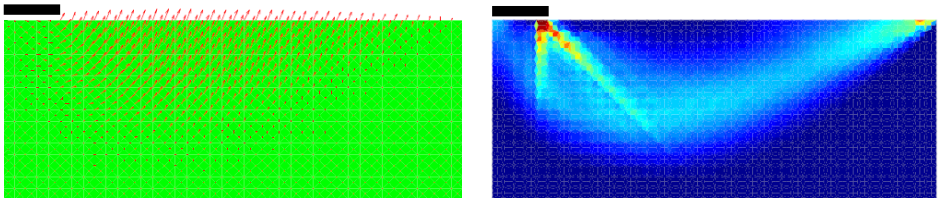

Figure 5.3 Patterns of plastic energy dissipation and velocity field $\varphi' = 40^0$

Bearing capacity factor *Nγ*

In this paper, we also carried out numerical solutions for the determination of bearing capacity factor N_γ. The problem is checked with two conditions: for smooth and rough footing.

Bearing capacity factor N_γ for smooth footing behaviour

The illustration of this problem is shown in Figure 6. Using mesh of 16404 elements formulated by NS-FEM procedure, we also compare N_γ values with solutions given by other authors (Meyerhof & Hanna, 1978; Michalowski, 1995; Davis & Booker, 1973).

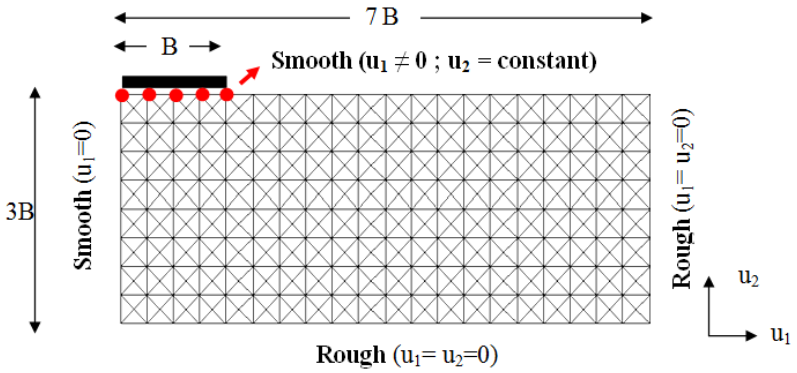

Figure 6: Meshing and boundary conditions for smooth footing

Results of this problem are solved for several cases of internal friction angle $\varphi' = 5 \div 40^0$ and presented in Table 3 and Figure 7.

Table 3: Comparing bearing capacity N_γ in drained condition

$\varphi'(^0)$	Bearing capacity factor N_γ				
	NS-FEM	**M. Hjiaj**	**Meyerhof**	**Botton**	**Michalowski**
5	0.0905	0.092	0.035	0.09	0.127
10	0.2940	0.298	0.183	0.29	0.423
15	0.7212	0.720	0.565	0.71	1.050
20	1.6129	1.602	1.435	1.6	2.332
25	3.5072	3.490	3.383	3.51	5.02
30	7.6938	7.696	7.834	7.74	10.918
35	17.5410	17.668	18.5776	17.8	24.749
40	42.8626	43.707	46.845	44	60.215

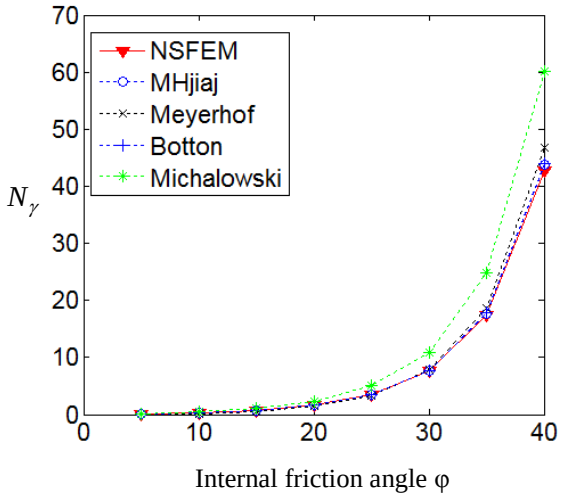

Figure 7: Bearing capacity N_γ for smooth footing behaviour

Bearing capacity factor Nγ for rough footing behaviour

The illustration of this problem is shown in Figure 8. Using mesh of 16404 elements formulated by NS-FEM procedure, we also compare N_γ values with solutions given by other authors (Meyerhof & Hanna, 1978; Michalowski, 1995; Davis & Booker, 1973).

Results of this problem are solved for several cases of internal friction angle $\varphi' = 5 \div 40^0$ and presented in Table 4 and Figure 9.

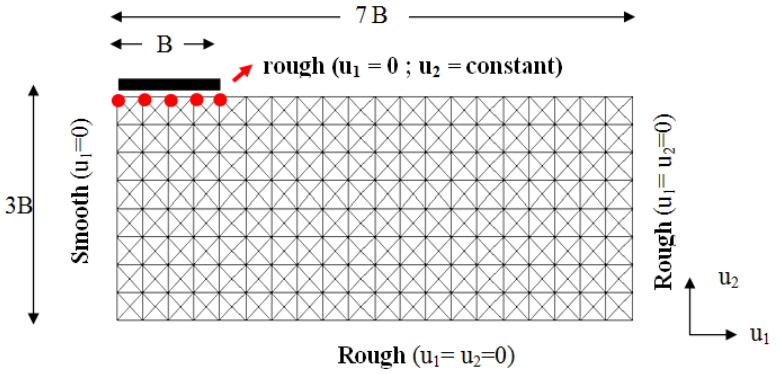

Figure 8: Meshing and boundary conditions for rough footing

Table 4: Bearing capacity factor Nγ

$\varphi'(^0)$	Bearing capacity factor N_γ							
	NS-FEM	**M. Hjiaj**	**Meyer hof**	**Hansen**	**Vesic**	**Booker**	**Kumar**	**Micha lowski**
5	0.1345	0.122	0.070	0.075	0.14	0.244	0.230	0.181
10	0.4712	0.455	0.367	0.389	1.22	0.563	0.690	0.706
15	1.2281	1.210	1.129	1.182	2.64	1.301	1.600	1.938
20	2.8784	2.857	2.871	2.948	5.38	3.007	3.430	4.468
25	6.4116	6.463	6.766	6.758	10.8	6.950	7.180	9.765
30	14.337	14.621	15.667	15.070	22.4	16.064	15.57	21.39
35	33.470	34.163	37.152	33.921	48.0	37.126	35.16	48.68
40	86.746	85.110	93.691	79.541	109.	85.805	85.73	118.8

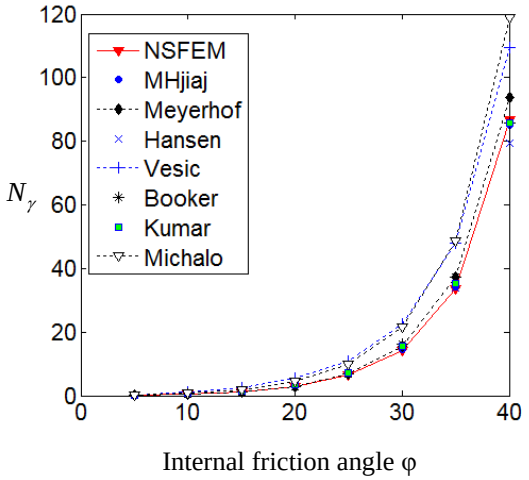

Figure 9: Meshing and boundary conditions for rough footing.

CONCLUSION

An innovative procedure for upper bound limit analysis based on node-based smoothed finite element method and second order cone programming has been described.

SOCP is a powerful technique for non-linear optimisation that allows us to obtain accurate solutions for many difficult geotechnical problems. This is mainly because of the advantage of this method using NS-FEM which are numerical problems constructed without any mapping technique for all types of elements. Using this advantage, we will overcome the deterioration in the accuracy of the solution of

many geotechnical problems where element mesh is heavily distorted. Besides, the application of NS-FEM for upper bound limit analysis promises savings in computer resources, and large scale problems can be solve accurately with reduced amount of time. Dealing with these types of problems is part of our on-going project.

REFERENCES

Chen, W.F. (1975). *Limit analysis and soil plasticity*. Amsterdam: Elsevier.

Davis, E. H., and Booker, J. R. (1993). Some adaptations of classical plasticity theory for soil stability problems. *Proceedings of the Symposium on the Role of Plasticity in Soil Mechanics*: pp.24-41. Cambridge. England.

Le, C.V, Gilbert, M. and Askes, H. (2009). Limit analysis of plates using the EFG method and second-order cone programming. *International Journal for Numerical Methods in Engineering*, 78, 1532-1552.

Le, C.V., Askes, H. and Gilbert, M. (2010). Adaptive Element-Free Galerkin method applied to the limit analysis of plates. *Computer Methods in Applied Mechanics and Engineering*, 199, 2487 – 2496.

Le, C.V., Nguyen-Xuan, H. and Nguyen-Dang, H. (2010). Upper and lower bound limit analysis of plates using FEM and second-order cone programming. *Computers and Structures*, 88, 65 – 73.

Liu, G.R. and Nguyen Thoi Trung. (2010). *Smoothed Finite Element Methods*. CRC-Press.

Meyerhof, G.G. and Hanna, A.M. (1978). Ultimate bearing capacity of foundations on layered under inclined load. *Canadian Geotechnical Journal*, 15, 565-572.

Michalowski, R. L. BS. (1995). Slope stability analysis: a kinematical approach. *Geotechnique*, 45(2), 283-293.

Mosek. (2011).The MOSEK optimization toolbox for MATLAB manual. version 6.0 edition. Retrieved 2011, from http://www.mosek.com.

Prandtl, L. (1920). Ueber die haerte plastischer koerper. Nachrichtex der Akademie der Wissenschaften in Gottingen. II. Mathematisch-Physikalische Klasse II, 12, 74-85.

Sloan, S.W. and Kleeman, P.W. (1995). Upper bound limit analysis using discontinuous velocity fields. *Computer Methods in Applied Mechanics and Engineering*, 127, 293-314.